A Numerical Study of Instability Arising from the Bénard Problem

by

Yuwei Zhao

A research paper
presented to the University of Waterloo
in partial fulfillment of the
requirement for the degree of
Master of Mathematics
in
Computational Mathematics

Supervisor: Prof. Justin W.L. Wan & Prof. Serge J.D. D'Alessio

Waterloo, Ontario, Canada, 2012

I hereby declare that I am the sole author of this report. This is a true copy of the report, including any required final revisions, as accepted by my examiners.

I understand that my report may be made electronically available to the public.

Abstract

Investigated in this report is the Rayleigh-Bénard problem with rotation and a periodic temperature distribution. Both approximate and numerical solutions to the steady-state and unsteady equations have been obtained. The numerical results are based on a finite difference method together with an implicit time stepping method and an iteration algorithm. The analytical results, on the other hand, were obtained by expanding the variables in a series involving a small parameter appearing in the governing equations. Comparisons between the numerical and the analytical results are also included. By varying the Rayleigh number the numerical results were able to confirm the theoretical prediction for when the flow becomes unstable.

Acknowledgements

I am deeply thankful to my supervisors, Prof. Justin W.L. Wan and Prof. Serge J.D. D'Alessio, for their guidance through this project. They have been always patient while giving me the insights to tackle tasks with enthusiasm. I would also like to thank my family for their love and my friends for their help.

Dedication

This is dedicated to my mother, Lei Zhao.

Table of Contents

List of Tables

List of Figures

Chapter 1

Introduction

By investigating the convection of air, meteorologists can obtain valuable information to aid them in the prediction of weather as well as the study of climate. Our motivation is to study air convection in the atmosphere, shown in Figure 1.1. The diagram presents key features which are used in describing the general circulation observed in the atmosphere. For example, it shows a decreasing surface temperature towards the pole due to solar heating and rotation about the polar axis. The thickness of the atmosphere is denoted by H and is small compared to the radius of the earth, R. The ratio $\frac{H}{R}$ is denoted by δ which is a small parameter.

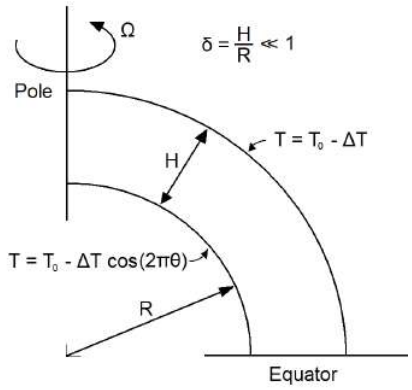

Figure 1.1: The flow setup by a simpler geometry

In this report, we will investigate a simplified version of that shown in Figure 1.1. We will consider a similar problem in a rectangular coordinate system, that of free convection confined within a long, rotating rectangular domain with a sinusoidally varying temperature along the bottom. This simplified problem can be thought of as an extension of traditional Rayleigh-Bénard convection. Rayleigh-Bénard convection has been thoroughly studied and is very well understood [1]. In the original Rayleigh-Bénard experiment [2], a horizontal fluid layer is confined within two thermally well conducting plates in parallel positions. When the temperature difference between the top and bottom plates is higher than a critical value, a flow develops and forms a series of convection cells. The difference between our problem and the traditional Bénard problem is that our problem includes both rotation and a periodic temperature distribution along the bottom plate.

Numerous investigations have been devoted to the Bénard problem and many of them are documented in the review by Bodenschatz, Pesch and Ahlers [1]. A recent study worth mentioning is that of Freund, Pesch and Zimmermann[3] which investigates Bénard convection with a sinusoidal temperature boundary condition, but without rotation. Our problem is an extension of their work to include rotation.

In this project, approximate steady and unsteady analytical solutions have been obtained by D'Alessio and Ogden [4] by taking advantage of the thinness of the fluid layer when the governing equations are cast in dimensionless form. Numerical solutions have been computed and one goal of this research is to compare the approximate steady and unsteady analytical solutions with the numerical solutions. Another objective is to propose an efficient numerical solution procedure to solve the full system of equations. Another goal of this project is to conduct numerous numerical experiments showing the evolution of convective flows with increasing Rayleigh (Ra) number.

The remainder of this report is arranged as followings. Chapter 2 contains background information on the Bénard problem and introduces the full system of governing equations. Chapter 3 describes the numerical solution procedure used to solve the governing equations. Chapter 4 presents numerical results and comparisons with analytical results that was derived in Chapter 2. In Chapter 5, we summarizes the key results.

Chapter 2

Model

2.1 Traditional Bénard problem

Traditional Bénard convection is also referred to as Rayleigh-Bénard convection. In a thermally expansive fluid, hot fluid rises whereas cold fluid sinks. Rayleigh-Bénard convection concerns the study of the instabilities which gives rise to fluid motion.

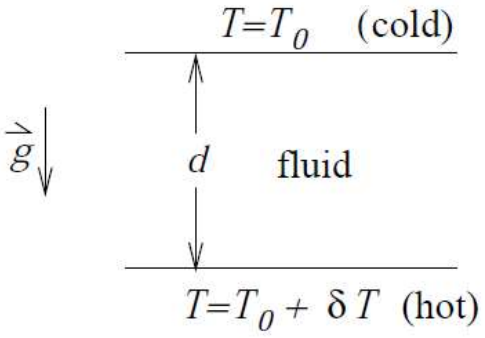

Figure 2.1: Rayleigh-Bénard convection.

When there is no convection, that is, no movement of fluid, the temperature gradient should be constant. δT is the temperature difference between the bottom and the top of

the fluid layer. If δT is small, then there will be no convection , due to the stabilizing effect of viscosity. But if δT is sufficiently large, then convection will occur.

2.2 Governing equations for Bénard problem with rotation and a periodic temperature distribution

Although we are primarily interested in solving the problem on the globe, here we simplify the problem to a thin rectangular domain. The main difference between this problem and the traditional Bénard problem is that this problem includes rotation and a periodic temperature distribution on the bottom plate.

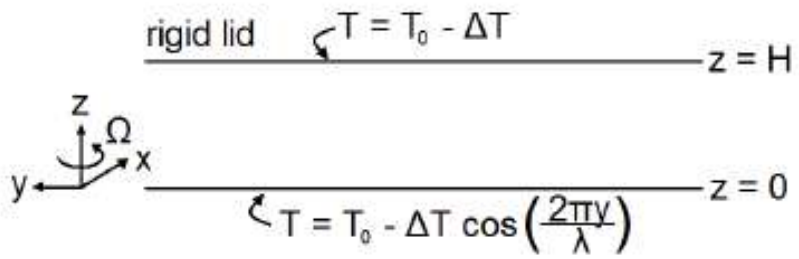

Figure 2.2: The coordinate system and configuration.

The above figure shows the two-dimensional flow is constricted within a thin rectangular area. Our assumption is that the flow is uniform in the x-direction and the entire configuration can rotate about the z-axis .

According to conservation of mass, momentum and energy, we obtain the following governing equations (the interested readers may find more details of these equations in [5]):

$$\vec{\nabla} \cdot \vec{v} = 0 \tag{2.1}$$

$$\frac{\partial \vec{v}}{\partial t} + \left(\vec{v} \cdot \vec{\nabla}\right) \vec{v} + f\hat{k} \times \vec{v} = \frac{-1}{\rho_0}\vec{\nabla} p - \frac{\rho}{\rho_0} g\hat{k} + \nu \nabla^2 \vec{v}, \tag{2.2}$$

$$\frac{\partial T}{\partial t} + \left(\vec{v} \cdot \vec{\nabla}\right) T = \kappa \nabla^2 T, \tag{2.3}$$

where $\vec{\nabla} = (\partial_x, \partial_y, \partial_z)$, $\nabla^2 = \partial^2_{xx} + \partial^2_{yy} + \partial^2_{zz}$, $\vec{v} = (u, v, w)$ is the velocity, T is the temperature, $\hat{k}$ is the unit vector in the z-direction, or $\hat{k} = (0, 0, 1)$, $\vec{\Omega} = (f/2)\hat{k}$ is the vector denoting the rate of rotation, thus f denotes the twice of the rate of rotation, $\vec{g} = -g\hat{k}$ is the acceleration due to gravity, p is the pressure, and ν and κ are two fluid properties which represent the kinematic viscosity and the thermal diffusivity, respectively. Here, the density ρ, is taken to vary with temperature according to

$$\rho = \rho_0(1 - \alpha\,[T - T_0]),$$

with α representing the thermal expansion coefficient and ρ_0, T_0 representing reference values for density and temperature.

From equation (2.1), we have that

$$\frac{\partial u}{\partial x} + \frac{\partial v}{\partial y} + \frac{\partial w}{\partial z} = 0. \tag{2.4}$$

Because the flow is assumed to be uniform in the x-direction, this means that $\frac{\partial u}{\partial x} = 0$. Therefore, a stream function ψ can be permitted, which is defined as:

$$v = \frac{\partial \psi}{\partial z} \text{ and } w = -\frac{\partial \psi}{\partial y}.$$

We can verify that equation (2.4) is satisfied after introducing the stream function ψ:

$$\frac{\partial u}{\partial x} + \frac{\partial v}{\partial y} + \frac{\partial w}{\partial z} = \frac{\partial v}{\partial y} + \frac{\partial w}{\partial z} = \frac{\partial}{\partial y}\left(\frac{\partial \psi}{\partial z}\right) + \frac{\partial}{\partial z}\left(-\frac{\partial \psi}{\partial y}\right) = 0.$$

In fluid dynamics, vorticity is a vector field and is defined as the curl of the velocity field: $\vec{\omega} = \vec{\nabla} \times \vec{v} = (\frac{\partial w}{\partial y} - \frac{\partial v}{\partial z}, -\frac{\partial w}{\partial x} + \frac{\partial u}{\partial z}, \frac{\partial v}{\partial x} - \frac{\partial u}{\partial y})$. According to our assumption that the flow is uniform in the x-direction, the first derivatives of v and w with respect to x are both zero. Therefore, $\vec{\omega} = \vec{\nabla} \times \vec{v} = (\frac{\partial w}{\partial y} - \frac{\partial v}{\partial z}, \frac{\partial u}{\partial z}, -\frac{\partial u}{\partial y})$. We can see here the last two components of $\vec{\omega}$ are only related to u. But we can derive the equation for u directly from equation

(2.2). And thus, we only need to look at the x-component of the vortocity $\vec{\omega}$, denoted as $\zeta = \frac{\partial w}{\partial y} - \frac{\partial v}{\partial z} = \frac{\partial}{\partial y}(-\frac{\partial \psi}{\partial y}) - \frac{\partial}{\partial z}(\frac{\partial \psi}{\partial z}) = -\left(\frac{\partial^2 \psi}{\partial y^2} + \frac{\partial^2 \psi}{\partial z^2}\right)$.

Right now, our system of equations has four unknowns, which are T, u, ψ, ζ. In order to solve for these four unknowns, we need four equations.

Using $\frac{\partial T}{\partial x} = 0$ and $\frac{\partial^2 T}{\partial x^2} = 0$ from our assumption that the flow is uniform in the x-direction and introducing ψ, the equation of T becomes

$$\frac{\partial T}{\partial t} + \frac{\partial \psi}{\partial z}\frac{\partial T}{\partial y} - \frac{\partial \psi}{\partial y}\frac{\partial T}{\partial z} = \kappa\left(\frac{\partial^2 T}{\partial y^2} + \frac{\partial^2 T}{\partial z^2}\right).$$

Similarly, the equation for u becomes:

$$\frac{\partial u}{\partial t} + \frac{\partial \psi}{\partial z}\frac{\partial u}{\partial y} - \frac{\partial \psi}{\partial y}\frac{\partial u}{\partial z} - f\frac{\partial \psi}{\partial z} = \nu\left(\frac{\partial^2 u}{\partial y^2} + \frac{\partial^2 u}{\partial z^2}\right).$$

Recall that the equation for ψ is:

$$\zeta = -\left(\frac{\partial^2 \psi}{\partial y^2} + \frac{\partial^2 \psi}{\partial z^2}\right).$$

In order to obtain the equation for ζ, we take the curl of equation (2.2); the first term on the left-hand side yields:

$$\vec{\nabla} \times \frac{\partial \vec{v}}{\partial t} = \frac{\partial(\vec{\nabla} \times \vec{v})}{\partial t} = \frac{\partial \vec{\omega}}{\partial t},$$

by the definition of vorticity. Because the x-component of the above involves ζ and we are aiming to derive the equation for ζ, we only need to look at the x-component of each term after taking the curl of equation (2.2).The term

$$\vec{\nabla} \times \left[(\vec{v} \cdot \vec{\nabla})\vec{v}\right] = \vec{\nabla} \times \left(v\frac{\partial u}{\partial y} + w\frac{\partial u}{\partial z}, v\frac{\partial v}{\partial y} + w\frac{\partial v}{\partial z}, v\frac{\partial w}{\partial y} + w\frac{\partial w}{\partial z}\right),$$

has an x-component given by:

$$\frac{\partial}{\partial y}(v\frac{\partial w}{\partial y} + w\frac{\partial w}{\partial z}) - \frac{\partial}{\partial z}(v\frac{\partial v}{\partial y} + w\frac{\partial v}{\partial z}) = \frac{\partial \psi}{\partial z}\frac{\partial \zeta}{\partial y} - \frac{\partial \psi}{\partial y}\frac{\partial \zeta}{\partial z}.$$

The x-component of $\vec{\nabla} \times (f\hat{k} \times \vec{v})$ is $-f\frac{\partial u}{\partial z}$. Therefore, the left-hand side is given by:

$$\frac{\partial \zeta}{\partial t} + \frac{\partial \psi}{\partial z}\frac{\partial \zeta}{\partial y} - \frac{\partial \psi}{\partial y}\frac{\partial \zeta}{\partial z} - f\frac{\partial u}{\partial z}.$$

Simplifying the right-hand side using vector identities, we obtain the equation for ζ:

$$\frac{\partial \zeta}{\partial t} + \frac{\partial \psi}{\partial z}\frac{\partial \zeta}{\partial y} - \frac{\partial \psi}{\partial y}\frac{\partial \zeta}{\partial z} - f\frac{\partial u}{\partial z} = -\alpha g\frac{\partial T}{\partial y} + \nu(\frac{\partial^2 \zeta}{\partial y^2} + \frac{\partial^2 \zeta}{\partial z^2}).$$

In conclusion, the system of equations is as follows:

$$\begin{aligned}
\frac{\partial \zeta}{\partial t} + \frac{\partial \psi}{\partial z}\frac{\partial \zeta}{\partial y} - \frac{\partial \psi}{\partial y}\frac{\partial \zeta}{\partial z} - f\frac{\partial u}{\partial z} &= -\alpha g\frac{\partial T}{\partial y} + \nu(\frac{\partial^2 \zeta}{\partial y^2} + \frac{\partial^2 \zeta}{\partial z^2}),\\
-\left(\frac{\partial^2 \psi}{\partial y^2} + \frac{\partial^2 \psi}{\partial z^2}\right) &= \zeta,\\
\frac{\partial u}{\partial t} + \frac{\partial \psi}{\partial z}\frac{\partial u}{\partial y} - \frac{\partial \psi}{\partial y}\frac{\partial u}{\partial z} - f\frac{\partial \psi}{\partial z} &= \nu\left(\frac{\partial^2 u}{\partial y^2} + \frac{\partial^2 u}{\partial z^2}\right),\\
\frac{\partial T}{\partial t} + \frac{\partial \psi}{\partial z}\frac{\partial T}{\partial y} - \frac{\partial \psi}{\partial y}\frac{\partial T}{\partial z} &= \kappa\left(\frac{\partial^2 T}{\partial y^2} + \frac{\partial^2 T}{\partial z^2}\right),
\end{aligned}$$

with boundary conditions given by:

$$\begin{aligned}
&u = v = w = \psi = \zeta = 0 && at \quad z = 0, H \ and \ y = 0, \lambda\\
&T = T_0 - \Delta T\cos\left(2\pi\frac{y}{\lambda}\right) && at \ \ z = 0,\\
&T = T_0 - \Delta T && at \ \ z = H, \ y = 0, \lambda.
\end{aligned}$$

2.2.1 Nondimensionalization of equations

We introduce the non-dimensional quantities by using the following scaling:

$$t \to \frac{H^2}{k}t, y \to \lambda y, z \to Hz, \psi \to \kappa\psi, \zeta \to \frac{\kappa}{H^2}\zeta, T \to (T_0 - \Delta T) + \Delta T T, u \to \frac{\kappa}{H}u.$$

This procedure introduces the non-dimensional parameters:

$$Ra = \frac{\alpha g H^3 \Delta T}{\nu\kappa}, Ro = \frac{\kappa}{Hf\lambda}, Pr = \frac{\nu}{\kappa}, \delta = \frac{H}{\lambda}.$$

Note that the parameter Ra is called Rayleigh number and represents the ratio of buoyancy forces to viscous forces.When Ra exceeds a critical value, instability occurs.

Expressed in non-dimensional form, the system of equations becomes:

$$\frac{\partial \zeta}{\partial t} + \delta \frac{\partial \psi}{\partial z}\frac{\partial \zeta}{\partial y} - \delta \frac{\partial \psi}{\partial y}\frac{\partial \zeta}{\partial z} - \frac{\delta}{Ro}\frac{\partial u}{\partial z} = \delta Pr Ra \frac{\partial T}{\partial y} + Pr(\delta^2 \frac{\partial^2 \zeta}{\partial y^2} + \frac{\partial^2 \zeta}{\partial z^2}), \tag{2.5}$$

$$-\left(\delta^2 \frac{\partial^2 \psi}{\partial y^2} + \frac{\partial^2 \psi}{\partial z^2}\right) = \zeta, \tag{2.6}$$

$$\frac{\partial u}{\partial t} + \delta \left(\frac{\partial \psi}{\partial z}\frac{\partial u}{\partial y} - \frac{\partial \psi}{\partial y}\frac{\partial u}{\partial z}\right) - \frac{\delta}{Ro}\frac{\partial \psi}{\partial z} = Pr\left(\delta^2 \frac{\partial^2 u}{\partial y^2} + \frac{\partial^2 u}{\partial z^2}\right), \tag{2.7}$$

$$\frac{\partial T}{\partial t} + \delta \left(\frac{\partial \psi}{\partial z}\frac{\partial T}{\partial y} - \frac{\partial \psi}{\partial y}\frac{\partial T}{\partial z}\right) = \delta^2 \frac{\partial^2 T}{\partial y^2} + \frac{\partial^2 T}{\partial z^2}, \tag{2.8}$$

Boundary conditions for traditional Bénard problem are:

$$\begin{aligned} &\psi = \zeta = u = 0 && at \;\; z = 0, 1 \text{ and } y = 0, 1 \\ &T = 0 && at \;\; z = 1 \\ &T = 2(1 - z) && at \;\; y = 0, 1 \\ &T = 2 && at \;\; z = 0 \end{aligned} \tag{2.9}$$

while boundary conditions for Bénard problem with rotation and a periodic temperature distribution are given by:

$$\begin{aligned} &\psi = \zeta = u = 0 && at \;\; z = 0, 1 \text{ and } y = 0, 1 \\ &T = 0 && at \;\; z = 1 \text{ and } y = 0, 1 \\ &T = 1 - \cos(2\pi y) && at \;\; z = 0 \end{aligned} \tag{2.10}$$

We are mainly interested in solving equations (2.5) to (2.8) subject to the boundary conditions given by (3.5).

2.3 Analytical steady-state solutions

2.3.1 Analytical steady-state solutions for the traditional Bénard problem

It can be shown that the analytical steady-state stable solutions to the traditional Bénard problem is: $\zeta = \psi = 0, T = 2(1-z), u = 0$ [5].

2.3.2 Analytical steady-state solution for Bénard problem with rotation and a periodic temperature distribution

The steady-state solution to this problem is much more complicated than the traditional Bénard problem due to the periodic temperature distribution. Instead of solving the complete system of equations, we expand the variables in a series in the small parameter δ to get an approximate analytical solution.

For small δ ($\delta << 1$), we expand the variables in the following series:

$$\begin{aligned}
\psi &= \psi_0 + \delta\psi_1 + \dots, \\
\zeta &= \zeta_0 + \delta\zeta_1 + \dots, \\
u &= u_0 + \delta u_1 + \dots, \\
T &= T_0 + \delta T_1 + \dots.
\end{aligned}$$

Retaining only the dominant terms T_0, ζ_0, ψ_0, and u_0. Here, T_0, ζ_0, ψ_0, and u_0 correspond to the solutions to the complete system of equations when $\delta = 0$, *i.e.* $H = 0$. Then, the steady-state problem is governed by the system:

$$\frac{\partial^2 T_0}{\partial z^2} = 0, \tag{2.11}$$

$$\frac{\partial^2 \zeta_0}{\partial z^2} = -\delta Ra \frac{\partial T_0}{\partial y}, \tag{2.12}$$

$$\frac{\partial^2 \psi_0}{\partial z^2} = -\zeta_0, \tag{2.13}$$

$$\frac{\partial^2 u_0}{\partial z^2} = 0, \tag{2.14}$$

subject to boundary conditons (3.5).

If we denote the steady-state solutions to equations (2.11)-(2.14) by $T_s, \zeta_s, \psi_s, u_s$, the solutions can be found and are given by:[4]

$$T_s(y,z) = (1-z)[1-\cos(2\pi y)], \tag{2.15}$$
$$\psi_s(y,z) = 2\pi\delta RaF(z)\sin(z\pi y), \tag{2.16}$$
$$\zeta_s(y,z) = -2\pi\delta RaF''(z)\sin(2\pi y), \tag{2.17}$$
$$u_s(y,z) = 0, \tag{2.18}$$

where

$$F(z) = -\frac{1}{120}z^5 + \frac{1}{24}z^4 - \frac{1}{18}z^3 + \frac{1}{45}z, \tag{2.19}$$
$$F''(z) = -\frac{1}{6}z^3 + \frac{1}{2}z^2 - \frac{1}{3}z. \tag{2.20}$$

Since $u_s = 0$, this shows that rotation does not affect the steady-state solution at leading order.

2.4 Analytical unsteady solution for Bénard problem with rotation and a periodic temperature distribution

We use a similar technique as that for solving the steady-state problem. For small δ ($\delta \ll 1$), we expand the variables in the series.

Again, retaining the dominant terms in the unsteady equations leads to the simplified system:

$$\frac{\partial T_0}{\partial t} = \frac{\partial^2 T_0}{\partial z^2}, \tag{2.21}$$
$$\frac{\partial \zeta_0}{\partial t} = Pr\frac{\partial^2 \zeta_0}{\partial z^2} + Pr\delta Ra\frac{\partial T_0}{\partial y}, \tag{2.22}$$
$$\frac{\partial^2 \psi_0}{\partial z^2} = -\zeta_0, \tag{2.23}$$
$$\frac{\partial u_0}{\partial t} = Pr\frac{\partial^2 u_0}{\partial z^2}, \tag{2.24}$$

subject to boundary conditions (3.5) and the initial conditions: $T_0 = T(y, z, t = 0) = T_s(y, z)$, $\zeta_0 = \zeta_s(y, z)$, $\psi_0 = \psi_s(y, z)$, $u_0 = u_s(y, z) = 0$.

Since we use the initial condition $T_0 = T(y, z, t = 0) = T_s(y, z)$, it follows that $T = T_s$ for all $t > 0$.

Also, since $u_0 = u(y, z, t = 0) = u_s = 0$, then $u = u_s = 0$ for all $t > 0$.

To solve equation (2.22), we set $\zeta = \zeta_s + \hat{\zeta}$. Then, (2.22) simplifies to:

$$\frac{\partial \hat{\zeta}}{\partial t} = Pr \frac{\partial^2 \hat{\zeta}}{\partial z^2}, \tag{2.25}$$

subject to $\hat{\zeta} = 0$ along the boundary and $\hat{\zeta}(y, z, t = 0) = -\zeta_s(y, z)$ which corresponding to $\zeta = 0$ at $t = 0$.

By separation of variables, the general solution to equation (2.25) is:

$$\hat{\zeta}(y, z, t) = \sum_{n=1}^{\infty} a_n(y) e^{-n^2\pi^2 Prt} \sin(n\pi z).$$

To determine $a_n(y)$, we apply initial conditions and use orthogonality to obtain:

$$a_n(y) = -2 \int_0^1 \zeta_s(y, z) sin(n\pi z)\, dz = -\frac{4\delta Ra}{\pi^2 n^3} \sin(z\pi y).$$

Similarly, we set $\psi = \psi_s + \hat{\psi}$ and obtain

$$\frac{\partial^2 \hat{\psi}}{\partial z^2} = -\hat{\zeta},$$

with $\hat{\psi} = 0$ at $t = 0$.
Then, we find that

$$\hat{\psi}(y, z, t) = -\sum_{n=1}^{\infty} \frac{a_n(y)}{n^2\pi^2} e^{-n^2\pi^2 Prt} \sin(n\pi z).$$

Chapter 3

Numerical Methods

Recall that the full equations are given as:

$$\frac{\partial \zeta}{\partial t} + \delta \frac{\partial \psi}{\partial z}\frac{\partial \zeta}{\partial y} - \delta \frac{\partial \psi}{\partial y}\frac{\partial \zeta}{\partial z} - \frac{\delta}{Ro}\frac{\partial u}{\partial z} = \delta Pr Ra \frac{\partial T}{\partial y} + Pr(\delta^2 \frac{\partial^2 \zeta}{\partial y^2} + \frac{\partial^2 \zeta}{\partial z^2}), \tag{3.1}$$

$$-\left(\delta^2 \frac{\partial^2 \psi}{\partial y^2} + \frac{\partial^2 \psi}{\partial z^2}\right) = \zeta, \tag{3.2}$$

$$\frac{\partial u}{\partial t} + \delta \left(\frac{\partial \psi}{\partial z}\frac{\partial u}{\partial y} - \frac{\partial \psi}{\partial y}\frac{\partial u}{\partial z}\right) - \frac{\delta}{Ro}\frac{\partial \psi}{\partial z} = Pr\left(\delta^2 \frac{\partial^2 u}{\partial y^2} + \frac{\partial^2 u}{\partial z^2}\right), \tag{3.3}$$

$$\frac{\partial T}{\partial t} + \delta \left(\frac{\partial \psi}{\partial z}\frac{\partial T}{\partial y} - \frac{\partial \psi}{\partial y}\frac{\partial T}{\partial z}\right) = \delta^2 \frac{\partial^2 T}{\partial y^2} + \frac{\partial^2 T}{\partial z^2}, \tag{3.4}$$

and the boundary conditions for the Bénard problem with rotation and a periodic temperature distribution are given by:

$$\begin{aligned} &\psi = \zeta = u = 0 && at \;\; z = 0, 1 \text{ and } y = 0, 1 \\ &T = 0 && at \;\; z = 1 \text{ and } y = 0, 1 \\ &T = 1 - \cos(2\pi y) && at \;\; z = 0 \end{aligned} \tag{3.5}$$

In this chapter, we discuss the numerical methods to compute the numerical solutions for the full system of equations.

3.1 Finite difference method

In this project, we use the finite difference method [6] as the main numerical method [7] to compute the numerical solutions. The partial differential equations can be discretized using first order and second order finite difference schemes on a computational grid, as shown in Figure 3.1.

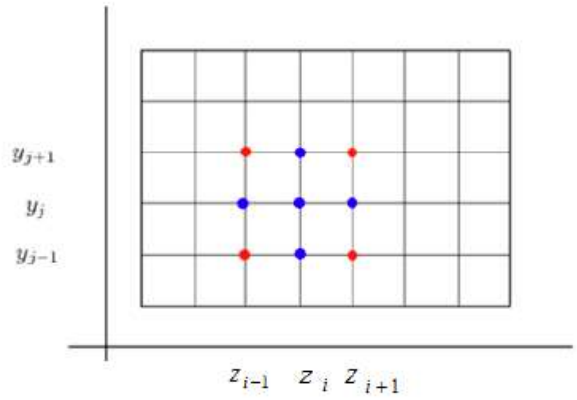

Figure 3.1: The finite difference method relies on discretizing a function on a grid

Let $N+1$ be the number of grid points along each direction. Thus the grid size $h = \frac{1}{N+1}$. A grid point is denoted by (z_i, y_j), where $z_i = ih, y_j = jh, 1 \leq i \leq N+1, 1 \leq j \leq N+1$. We approximate $T(z_i, y_j)$ by $T_{i,j}$ on grid point (z_i, y_j). Similarly, $\zeta_{i,j}$, $\psi_{i,j}$, and $u_{i,j}$ are approximations of $\zeta(z_i, y_j)$, $\psi(z_i, y_j)$, and $u(z_i, y_j)$, respectively.

Then, we discretize each term in the system. We will focus on equation (3.4) as an example.

$$\left(\frac{\partial T}{\partial z}\right)_{i,j} = \frac{T_{i+1,j} - T_{i-1,j}}{2h} + \mathcal{O}(h^2), \tag{3.6}$$

$$\left(\frac{\partial T}{\partial y}\right)_{i,j} = \frac{T_{i,j+1} - T_{i,j-1}}{2h} + \mathcal{O}(h^2), \tag{3.7}$$

$$\left(\frac{\partial^2 T}{\partial y^2}\right)_{i,j} = \frac{T_{i,j-1} - 2T_{i,j} + T_{i,j+1}}{h^2} + \mathcal{O}(h^2), \tag{3.8}$$

$$\left(\frac{\partial^2 T}{\partial z^2}\right)_{i,j} = \frac{T_{i-1,j} - 2T_{i,j} + T_{i+1,j}}{h^2} + \mathcal{O}(h^2). \tag{3.9}$$

The derivatives of the other functions are discretized similarly.

We note that one sided difference is used at the end points. Consider (3.4) again. When discretizing the equation of T, we use forward difference approximation at $j = 1$, which is given by:

$$\left(\frac{\partial T}{\partial y}\right)_{i,1} = \frac{T_{i,2} - T_{i,1}}{h} + \mathcal{O}(h).$$

We use backward difference approximation at $j = N + 1$, which is given by:

$$\left(\frac{\partial T}{\partial y}\right)_{i,N+1} = \frac{T_{i,N+1} - T_{i,N}}{h} + \mathcal{O}(h).$$

The finite difference approximation in space for the numerical approximation of (3.4) without discretizing $\frac{\partial T}{\partial t}$ is:

$$\begin{aligned}&\frac{\partial T}{\partial t} + \delta(\frac{\psi_{i+1,j} - \psi_{i-1,j}}{2h}\frac{T_{i,j+1} - T_{i,j-1}}{2h} - \frac{\psi_{i,j+1} - \psi_{i,j-1}}{2h}\frac{T_{i+1,j} - T_{i-1,j}}{2h})\\ &= \delta^2\frac{T_{i,j-1} - 2T_{i,j} + T_{i,j+1}}{h^2} + \frac{T_{i-1,j} - 2T_{i,j} + T_{i+1,j}}{h^2}.\end{aligned}$$

3.2 Implicit time stepping

When discretizing the terms involving time t in the system of equations, *i.e.* terms such as $\frac{\partial T}{\partial t}$, we apply the implicit time stepping method. Implicit method is used instead of explicit method since the explicit time stepping method requires a small Δt due to the stability condition. The implicit scheme, on the other hand, is stable for any Δt. Let $T^n_{i,j}$ be an approximation to $T(z_i, y_j)$ at time t^n. Then the implicit time stepping formula for the numerical approximation of equation (3.4) is :

$$\begin{aligned}\frac{T^{n+1}_{i,j} - T^n_{i,j}}{\Delta t} &= \delta^2\frac{T^{n+1}_{i,j-1} - 2T^{n+1}_{i,j} + T^{n+1}_{i,j+1}}{h^2} + \frac{T^{n+1}_{i-1,j} - 2T^{n+1}_{i,j} + T^{n+1}_{i+1,j}}{h^2}\\ &\quad - \delta(\frac{\psi^{n+1}_{i+1,j} - \psi^{n+1}_{i-1,j}}{2h}\frac{T^{n+1}_{i,j+1} - T^{n+1}_{i,j-1}}{2h} - \frac{\psi^{n+1}_{i,j+1} - \psi^{n+1}_{i,j-1}}{2h}\frac{T^{n+1}_{i+1,j} - T^{n+1}_{i-1,j}}{2h}). \qquad (3.10)\end{aligned}$$

The idea of implicit time stepping method is that we approximate all the terms involving time by their value at time $n + 1$.

We now derive the matrix form of the equation (3.10). Define:

$$\begin{aligned}(T^{n+1})' &= (T^{n+1}_{2,2}, T^{n+1}_{2,3}, \cdots, T^{n+1}_{2,N}, T^{n+1}_{3,2}, \cdots, T^{n+1}_{3,N}, \cdots, T^{n+1}_{N,2}, \cdots, T^{n+1}_{N,N}),\\ (T^n)' &= (T^n_{2,2}, T^n_{2,3}, \cdots, T^n_{2,N}, T^n_{3,2}, \cdots, T^n_{3,N}, \cdots, T^n_{N,2}, \cdots, T^n_{N,N}).\end{aligned}$$

According to the boundary conditions, $T = 0$ at $z = 1$ and $y = 0, 1$, $T = 1 - \cos(2\pi y)$ at $z = 0$. Thus, we have $T_{N+1,2} = T_{N+1,3} = \cdots = T_{N+1,N} = 0$, $T_{1,j} = 1 - \cos(2\pi y(j))$, for $j = 1 \cdots N + 1$. And $T_{i,1} = T_{i,N+1} = 0$, for $i = 2 \cdots N$. Similarly,

$$(\psi^{n+1})' = (\psi^{n+1}_{2,2}, \psi^{n+1}_{2,3}, \cdots, \psi^{n+1}_{2,N}, \psi^{n+1}_{3,2}, \cdots, \psi^{n+1}_{3,N}, \cdots, \psi^{n+1}_{N,2}, \cdots, \psi^{n+1}_{N,N}).$$

Consider the first derivative of T with respect to y,

$$\left(\frac{\partial T^{n+1}}{\partial y}\right)_{i,j} \approx \frac{T^{n+1}_{i,j+1} - T^{n+1}_{i,j-1}}{2h}.$$

The matrix form can be written as:

$$\frac{1}{2h}(Dy \times T^{n+1} + T_{RL}),$$

where the matrix Dy is to be defined and T_{RL} is a vector of size $(N-1)^2$ accounting for the boundaries of T. Since $T = 0$ at $y = 0$ and $y = 1$, we have

$$(T_{RL})' = (0, 0, \cdots, 0). \tag{3.11}$$

Let Dy_1 be an $(N-1) \times (N-1)$ matrix defined as:

$$Dy_1 = \begin{pmatrix} 0 & 1 & & & \\ -1 & 0 & 1 & & \\ & -1 & 0 & 1 & \\ & & \ddots & \ddots & \ddots \\ & & & -1 & 0 \end{pmatrix}.$$

Then the matrix Dy of size $(N-1)^2 \times (N-1)^2$ is given by:

$$Dy = \begin{pmatrix} Dy_1 & & & & \\ & Dy_1 & & & \\ & & Dy_1 & & \\ & & & \ddots & \\ & & & & Dy_1 \end{pmatrix}.$$

Similarly, the first derivative of T with respect to z can be written as:

$$\frac{1}{2h}(Dz \times T^{n+1} + T_{UD}),$$

where T_{UD} is a vector with size $(N-1)^2$, corresponding to the boundary values of T on the top and bottom,

$$(T_{UD})' = (-T_{1,2}, -T_{1,3}, \cdots, -T_{1,N}, 0, \cdots, 0).$$

Recall the boundary conditions stated above, we have $T_{1,j} = 1 - \cos(2\pi y(j))$, for $j = 2 \cdots N$. The matrix corresponding to the first derivative is defined as:

$$Dz_1 = \begin{pmatrix} 1 & & & & \\ & 1 & & & \\ & & 1 & & \\ & & & \ddots & \\ & & & & 1 \end{pmatrix}, \qquad Dz_2 = \begin{pmatrix} -1 & & & & \\ & -1 & & & \\ & & -1 & & \\ & & & \ddots & \\ & & & & -1 \end{pmatrix},$$

where Dz_1 and Dz_2 are both matrix with size $(N-1) \times (N-1)$. Then Dz is given by:

$$Dz = \begin{pmatrix} 0 & Dz_1 & & & \\ Dz_2 & 0 & Dz_1 & & \\ & Dz_2 & 0 & Dz_1 & \\ & & \ddots & \ddots & \ddots \\ & & & Dz_2 & 0 \end{pmatrix}.$$

The size of Dz is $(N-1)^2$ by $(N-1)^2$.

The approximation to the second derivative of T with respect to z is:

$$\left(\frac{\partial^2 T^{n+1}}{\partial z^2}\right)_{i,j} \approx \frac{T^{n+1}_{i-1,j} - 2T^{n+1}_{i,j} + T^{n+1}_{i+1,j}}{h^2}.$$

Its matrix form can be written as:

$$\frac{1}{h^2}(A \times T^{n+1} - T_{UD}),$$

where

$$A_1 = \begin{pmatrix} -2 & & & & \\ & -2 & & & \\ & & -2 & & \\ & & & \ddots & \\ & & & & -2 \end{pmatrix}, \qquad A_2 = \begin{pmatrix} 1 & & & & \\ & 1 & & & \\ & & 1 & & \\ & & & \ddots & \\ & & & & 1 \end{pmatrix},$$

and

$$A = \begin{pmatrix} A_1 & A_2 & & & \\ A_2 & A_1 & A_2 & & \\ & A_2 & A_1 & A_2 & \\ & & \ddots & \ddots & \ddots \\ & & & A_2 & A_1 \end{pmatrix}.$$

The size of both A_1 and A_2 is $N-1$ by $N-1$, and the size of A is $(N-1)^2 \times (N-1)^2$. The approximation to the second derivative of T with respect to y is:

$$\left(\frac{\partial^2 T^{n+1}}{\partial y^2}\right)_{i,j} \approx \frac{T^{n+1}_{i,j-1} - 2T^{n+1}_{i,j} + T^{n+1}_{i,j+1}}{h^2}.$$

Its matrix form can be written as:

$$\frac{1}{h^2}(B \times T^{n+1} - T_{RL}),$$

Since T_{RL} is a zero array (3.11),the matrix form can be rewritten as:

$$\frac{1}{h^2} B \times T^{n+1}.$$

Let

$$B_1 = \begin{pmatrix} -2 & 1 & & & \\ 1 & -2 & 1 & & \\ & 1 & -2 & 1 & \\ & & \ddots & \ddots & \ddots \\ & & & 1 & -2 \end{pmatrix}.$$

Then B is given by

$$B = \begin{pmatrix} B_1 & & & & \\ & B_1 & & & \\ & & B_1 & & \\ & & & \ddots & \\ & & & & B_1 \end{pmatrix}.$$

The size of B_1 is $(N-1) \times (N-1)$, and the size of B is $(N-1)^2 \times (N-1)^2$.

Similarly, the other terms on the right-hand side of equation (3.10) can be written as,

$$\begin{aligned}
\frac{T^{n+1}_{i,j+1} - T^{n+1}_{i,j-1}}{2h} &= \left(\frac{1}{2h} Dy \times T^{n+1}\right)_{i,j}, \\
\frac{T^{n+1}_{i+1,j} - T^{n+1}_{i-1,j}}{2h} &= \left(\frac{1}{2h}(Dz \times T^{n+1} + T_{UD})\right)_{i,j}, \\
\frac{\psi^{n+1}_{i,j+1} - \psi^{n+1}_{i,j-1}}{2h} &= \left(\frac{1}{2h} Dy \times \psi^{n+1}\right)_{i,j}, \\
\frac{\psi^{n+1}_{i+1,j} - \psi^{n+1}_{i-1.j}}{2h} &= \left(\frac{1}{2h} Dz \times \psi^{n+1}\right)_{i,j}.
\end{aligned}$$

Note that all the boundary values of ψ are zeros. Then we have

$$\begin{aligned}
T^{n+1} - T^n =& \Delta t \left(\delta^2 \frac{1}{h^2} B \times T^{n+1} + \frac{1}{h^2}(A \times T^{n+1} - T_{UD})\right) \\
&- \frac{\Delta t \delta}{4h^2}\left(diag(Dz \times \psi^{n+1}) \times (Dy \times T^{n+1}) - diag(Dy \times \psi^{n+1}) \times (Dz \times T^{n+1} + T_{UD})\right),
\end{aligned} \tag{3.12}$$

where $diag(Dz \times \psi^{n+1})$ is a diagonal matrix whose diagonal entries are $diag(Dz \times \psi^{n+1})_{ii} = (Dz \times \psi^{n+1})_i$, for $i = 1, \cdots, (N-1)^2$.

By arranging and combining terms in equation (3.12), we get:

$$\begin{aligned}
&T^{n+1} - \frac{\Delta t}{h^2}\left((\delta^2 B + A) - \frac{\delta}{4} diag(Dz \times \psi^{n+1}) \times Dy + \frac{\delta}{4} diag(Dy \times \psi^{n+1}) \times Dz\right) \times T^{n+1} \\
&= T^n - \frac{\Delta t}{h^2} T_{UD} + \frac{\Delta t \delta}{4h^2} diag(Dy \times \psi^{n+1}) \times T_{UD}.
\end{aligned}$$

Then the equation (3.10) can be written as:

$$A_T T^{n+1} = f^n_T,$$

where

$$\begin{aligned}
A_T &= I - \frac{\Delta t}{h^2}\left((\delta^2 B + A) - \frac{\delta}{4} diag(Dz \times \psi^{n+1}) \times Dy + \frac{\delta}{4} diag(Dy \times \psi^{n+1}) \times Dz\right), \\
f^n_T &= T^n - \frac{\Delta t}{h^2} T_{UD} + \frac{\Delta t \delta}{4h^2} diag(Dy \times \psi^{n+1}) \times T_{UD}.
\end{aligned}$$

A_T is the coefficient matrix of T^{n+1}, and it also depends on ψ^{n+1} which is also unknown. f^n_T is the sum of terms related to T^n and all the constant terms.

3.3 Iterative method

Recall that in the previous section, we can write equation (3.10) in the following form: $A_T T^{n+1} = f_T^n$. To emphasize A_T also depends on ψ^{n+1}, we rewrite it as:

$$A_T(\psi^{n+1})T^{n+1} = f_T^n.$$

Applying similar techniques, we can obtain matrix form of the other equations for ζ^{n+1}, ψ^{n+1}, and u^{n+1}, respectively. We start with solving the equation for temperature T first, since T is the driving force for the whole system. And the order of others does not matter. As a result, the system of equations can be written as the follows:

$$A_T(\psi^{n+1})T^{n+1} = f_T^n, \tag{3.13}$$
$$A_\zeta(T^{n+1}, \psi^{n+1}, u^{n+1})\zeta^{n+1} = f_\zeta^n, \tag{3.14}$$
$$A_\psi \psi^{n+1} = \zeta^{n+1}, \tag{3.15}$$
$$A_u(\psi^{n+1})u^{n+1} = f_u^n. \tag{3.16}$$

At time step $n+1$, we want to solve (3.13) to (3.16). But, all the equations are coupled. For instance, in order to solve equation (3.13) for T^{n+1}, we need to know the value of ψ^{n+1}. Apparently, ψ^{n+1} is also an unknown here. It is very complicated to solve all these four coupled equations directly. Instead, we apply a fixed point method here, Specially, we treat ψ^{n+1} as a fixed value. By fixing ψ^{n+1}, we can solve for T^{n+1}. Then we move on to the next equation, *i.e.* equation (3.14). Similarly, by fixing T^{n+1}, ψ^{n+1}, and u^{n+1}, we can solve for ζ^{n+1}. And then move on to the next, we solve for ψ^{n+1} by keeping ζ^{n+1} fixed. Lastly, we fix ψ^{n+1} and solve for u^{n+1}. Afterwards, we update the values of T^{n+1}, ζ^{n+1}, ψ^{n+1}, and u^{n+1} to the solutions we have obtained just now. Then we iterate the process until the differences of the value got from previous iteration and the value got in the current iteration are smaller than the tolerance ϵ we pick. After that, we move on to the next time step.

The previous paragraph gives a general idea of our iterative algorithm. When writing in a more precise way, we denote the k^{th} iteration of the solution at time step $n+1$ of T, ψ, ζ, u as $(\hat{T}^{n+1})^k$, $(\hat{\psi}^{n+1})^k$, $(\hat{\zeta}^{n+1})^k$, $(\hat{u}^{n+1})^k$, respectively. We begin with solving the equation for T. As described above, we need to fix the value of ψ in order to solve T. In the first iteration, we let $(\hat{\psi}^{n+1})^0 = \psi^n$, which means we fix ψ at the solution for ψ obtained from the previous time step. The general equation for T in iteration $k+1$ at time step $n+1$ is

$$A_T((\hat{\psi}^{n+1})^k)(\hat{T}^{n+1})^{k+1} = f_T^n. \tag{3.17}$$

Specially, in the first iteration of time step $t = \Delta t$, we fix ψ at its initial value. We can solve for $(\hat{T}^{n+1})^{k+1}$ from (3.17). Similarly, we can solve for $(\hat{\zeta}^{n+1})^{k+1}$, $(\hat{\psi}^{n+1})^{k+1}$, $(\hat{u}^{n+1})^{k+1}$.Then, we update the values of T^{n+1}, ζ^{n+1}, ψ^{n+1}, and u^{n+1} to $(\hat{T}^{n+1})^{k+1}$, $(\hat{\zeta}^{n+1})^{k+1}$, $(\hat{\psi}^{n+1})^{k+1}$, $(\hat{u}^{n+1})^{k+1}$, respectively. The iteration process terminates when the differences of the value got from previous iteration and the value got in the current iteration are smaller than a given tolerance ϵ. Note, we choose $\epsilon = 10^{-5}$ in our experiments.

The iteration algorithm is outlined in the following table:

Iteration Algorithm
1. Initialize $(\hat{T}^{n+1})^0 = T^n$, $(\hat{\zeta}^{n+1})^0 = \zeta^n$, $(\hat{\psi}^{n+1})^0 = \psi^n$,$(\hat{u}^{n+1})^0 = u^n$
$\rightarrow$ the solutions from the previous time step.
2. **for** $k = 0, 1, 2, \cdots$ until convergence achieved **do**
3. Solve for $(\hat{T}^{n+1})^{k+1}$ from $A_T((\hat{\psi}^{n+1})^k)(\hat{T}^{n+1})^{k+1} = f_T^n$
4. Solve for $(\hat{\zeta}^{n+1})^{k+1}$ from $A_\zeta((\hat{\psi}^{n+1})^k, (\hat{T}^{n+1})^k, (\hat{u}^{n+1})^k)(\hat{\zeta}^{n+1})^{k+1} = f_\zeta^n$
5. Solve for $(\hat{\psi}^{n+1})^{k+1}$ from $A_\psi(\hat{\psi}^{n+1})^{k+1} = (\hat{\zeta}^{n+1})^k$
6. Solve for $(\hat{u}^{n+1})^{k+1}$ from $A_u((\hat{\psi}^{n+1})^k)(\hat{u}^{n+1})^{k+1} = f_u^n$
7. **if** $\|(\hat{T}^{n+1})^{k+1} - (\hat{T}^{n+1})^k\|_\infty < \epsilon$ and $\|(\hat{\zeta}^{n+1})^{k+1} - (\hat{\zeta}^{n+1})^k\|_\infty < \epsilon$ and $\|(\hat{\psi}^{n+1})^{k+1} - (\hat{\psi}^{n+1})^k\|_\infty < \epsilon$ and $\|(\hat{u}^{n+1})^{k+1} - (\hat{u}^{n+1})^k\|_\infty < \epsilon$ **then** Terminate the iteration
8. **end if**
9. **end for**

Table 3.1: Iteration Algorithm

The unsteady solutions at the final time step of the full set of equations can be obtained by implementing algorithm in Table 3.1.

Chapter 4

Numerical Results

In this chapter, the numerical results obtained by applying the numerical methods in the previous chapter are presented. In our numerical experiments, we begin with comparing our numerical solutions with the analytical steady state solutions for the the approximated problem (2.11) to (2.14). Then, we compare the unsteady solutions with the analytical solutions for the simplified problem (2.21) to (2.24). Thereafter, we demonstrate the numerical solutions for the full set of original nonlinear system (2.5) to (2.8) with boundary conditions (3.5). Lastly, we show the evolution of the convection with increasing the Ra number and keeping other parameters constant. The calculations were performed on a Windows 7 laptop with 2.5GHZ processor, 4GB memory using MATLAB[8].

4.1 Numerical steady-state solutions of approximate equations

We will compare the numerical steady-state solutions of the approximate equation with the analytical solutions (2.15) to (2.20).

In this experiment, we pick $Ro = 0.0548$, $Pr = 0.7046$, and $Ra = 388.7$. The solutions are calculated using the grid size $N = 100$. In Figure 4.1 to Figure 4.4, numerical solutions are shown on the left-hand side and the analytical solutions are shown on the right-hand side. From the plots, it appears that the numerical methods we used have provided good agreement with the analytical solutions.

In order to convince the readers and ourselves of this, we present further comparisons of contour plots with different grid sizes for each unknown variable. In the steady-state

problem, both the numerical solutions and the analytical solutions for u are always zero. Thus, we omit the contour plot of u with different grid sizes. In the contour plots Figure 4.5 to Figure 4.7, the black curve in each plot is the analytical solution when grid size $h = \frac{1}{80}$. The yellow curve in each plot is the numerical solution when grid size $h = \frac{1}{10}$. The red curve in each plot is the numerical solution when grid size $h = \frac{1}{20}$. The green curve in each plot is the numerical solution when grid size $h = \frac{1}{40}$. The blue curve in each plot is the numerical solution when grid size $h = \frac{1}{80}$. We can see that with a smaller grid size, the numerical solutions provide better agreement with the analytical solution. Based on these plots, with the gird size $h = \frac{1}{80}$, the plot of the numerical solution is very close to the analytical solution. Therefore, we expect that a smaller grid size than $h = \frac{1}{80}$ would also provide a good approximation.

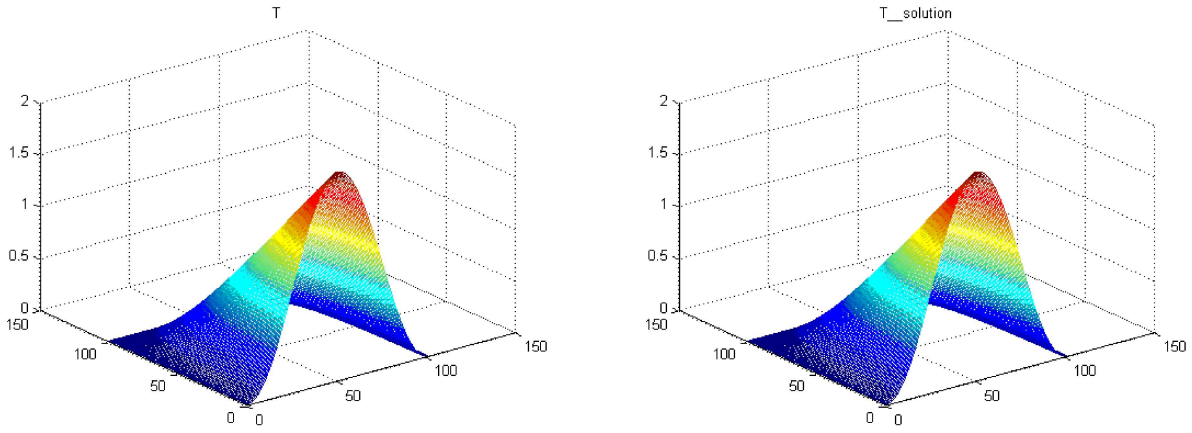

Figure 4.1: (Left): Numerical steady-state solution for T of approximate equations. (Right): Analytical steady-state solution for T of approximate equations.

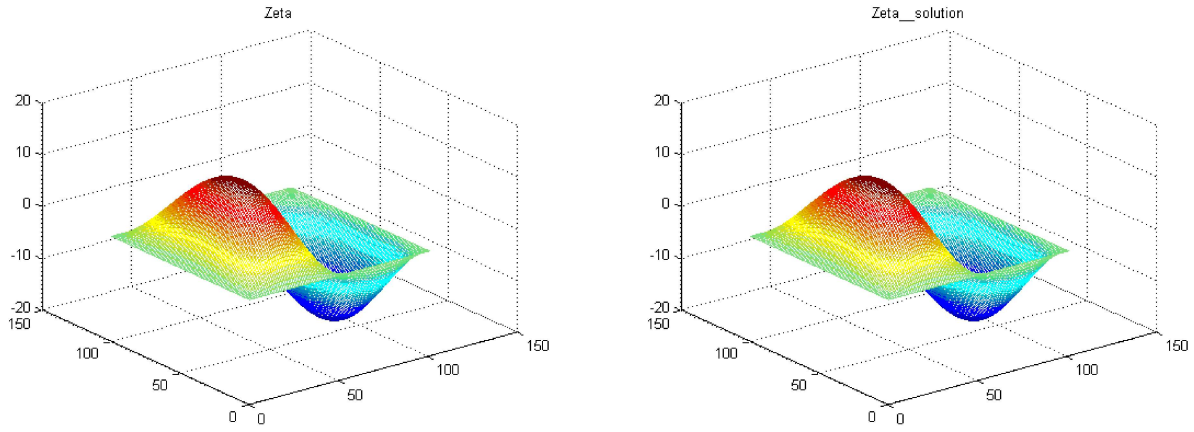

Figure 4.2: (Left): Numerical steady-state solution for ζ of approximate equations. (Right): Analytical steady-state solution for ζ of approximate equations.

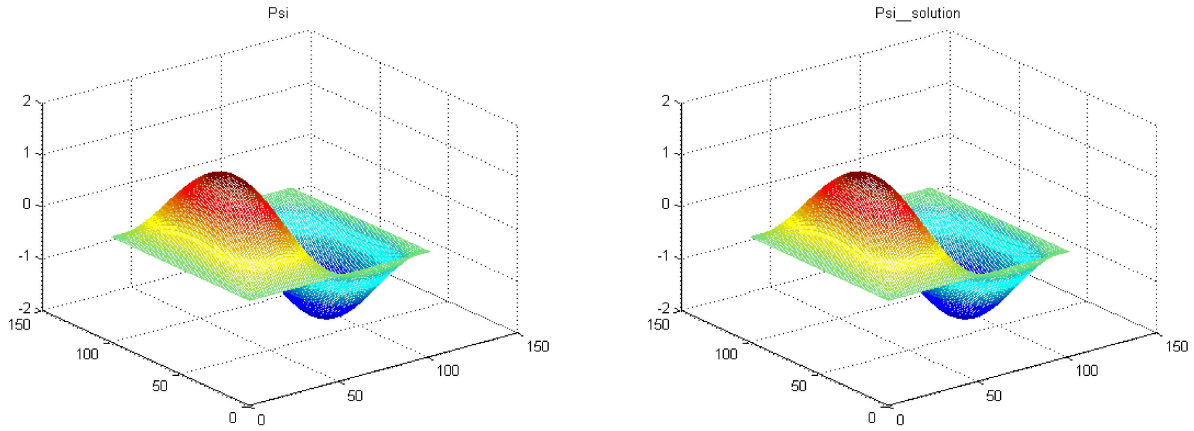

Figure 4.3: (Left): Numerical steady-state solution for ψ of approximate equations. (Right): Analytical steady-state solution for ψ of approximate equations.

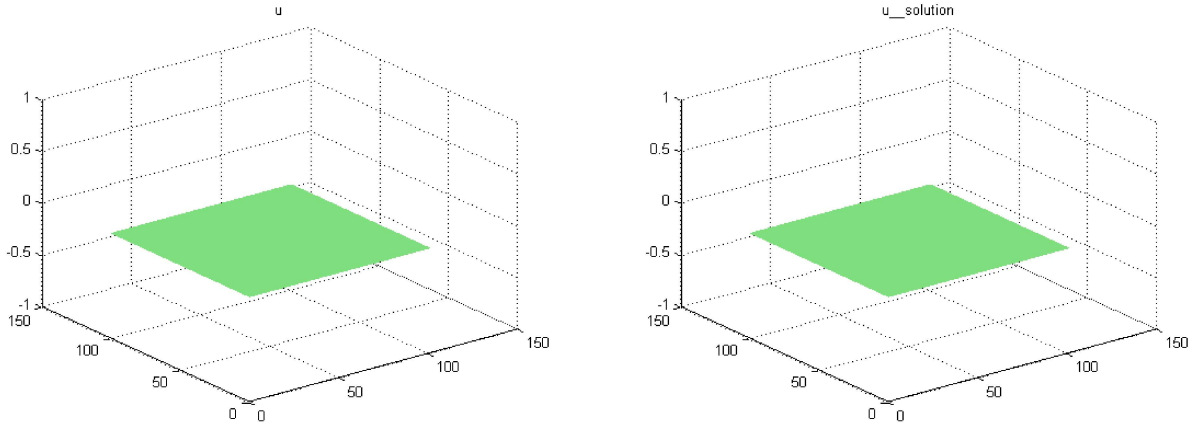

Figure 4.4: (Left): Numerical steady-state solution for u of approximate equations. (Right): Analytical steady-state solution for u of approximate equations.

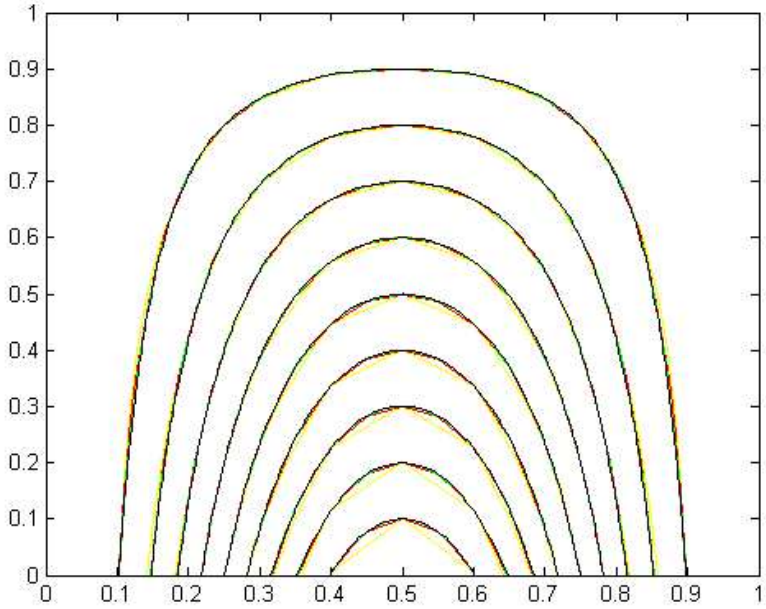

Figure 4.5: Contour plots of T with different grid sizes denoted by different colours. Yellow: $h = \frac{1}{10}$. Red: $h = \frac{1}{20}$. Green: $h = \frac{1}{40}$. Blue: $h = \frac{1}{80}$. Black: Analytical solution of T when grid size $h = \frac{1}{80}$

.

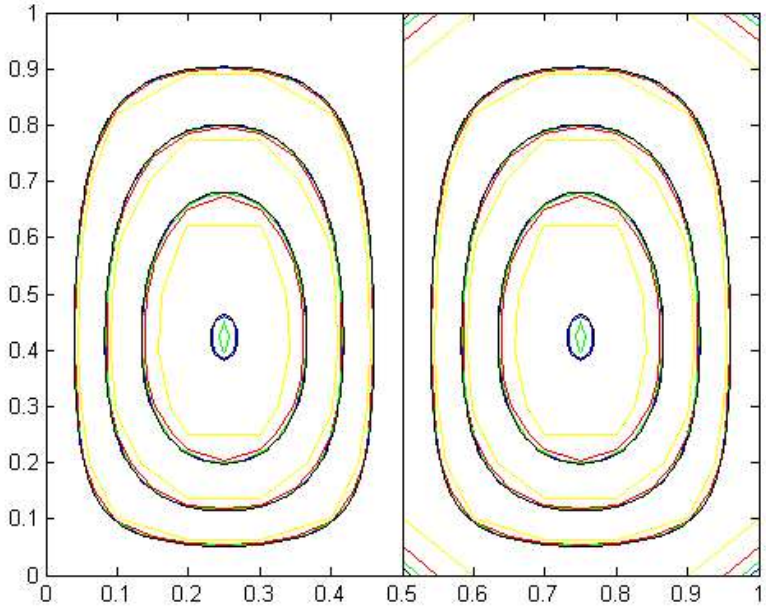

Figure 4.6: Contour plots of ζ with different grid sizes denoted by different colours. Yellow: $h = \frac{1}{10}$. Red: $h = \frac{1}{20}$. Green: $h = \frac{1}{40}$. Blue: $h = \frac{1}{80}$. Black: Analytical solution of ζ when grid size $h = \frac{1}{80}$

.

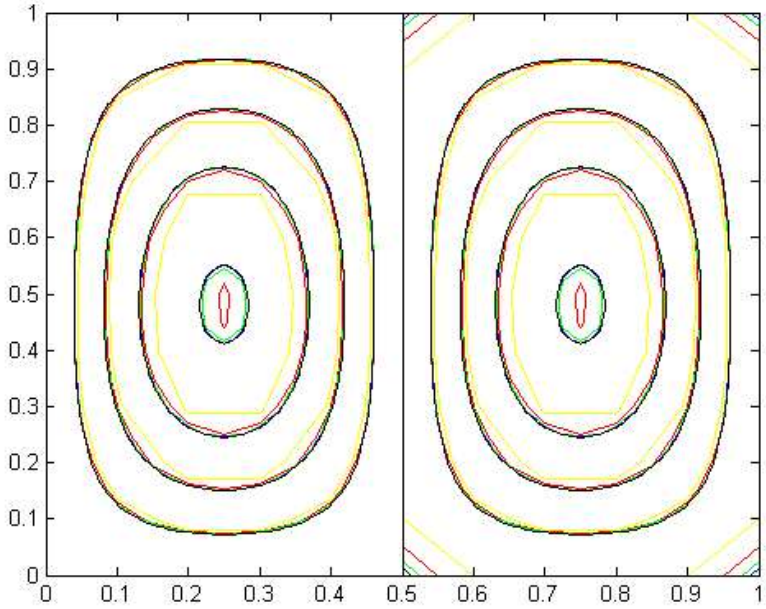

Figure 4.7: Contour plots of ψ with different grid sizes denoted by different colours. Yellow: $h = \frac{1}{10}$. Red: $h = \frac{1}{20}$. Green: $h = \frac{1}{40}$. Blue: $h = \frac{1}{80}$. Black: Analytical solution of ψ when grid size $h = \frac{1}{80}$

.

Table 4.1 displays the error calculated with varying grid sizes by defining E_h as the difference between the numerical solutions and the analytical solutions:

$$E(T)_h = \|T - T_s\|. \tag{4.1}$$

Similarly, we calculate the error for ψ, ζ, u, respectively. We can see the error of T is about 10^{-13}, which is essentially the roundoff error. In this simplified problem, the numerical solutions for T are actually the exact solution. Since $\frac{E_{2h}}{E_h}$ is approximately 4 for ζ and ψ, it demonstrates second order convergence, which is consistent with the error arising from the finite difference method we have discussed in the previous chapter (3.6) to (3.9).

grid size (h)	T		ζ		ψ	
	E_h	$\frac{E_{2h}}{E_h}$	E_h	$\frac{E_{2h}}{E_h}$	E_h	$\frac{E_{2h}}{E_h}$
$\frac{1}{10}$	0.0089×10^{-13}	$--$	0.0025	$--$	0.2219×10^{-3}	$--$
$\frac{1}{20}$	0.0200×10^{-13}	0.4444	0.0007	3.7483	0.0589×10^{-3}	3.7661
$\frac{1}{40}$	0.0222×10^{-13}	0.9000	0.0002	3.9760	0.0148×10^{-3}	3.9900
$\frac{1}{80}$	0.1021×10^{-13}	0.2174	0.0000	3.9963	0.0037×10^{-3}	3.9946

Table 4.1: Error table for numerical steady-state solutions of approximate problem.

4.2 Numerical unsteady solutions of approximate equations

In this experiment, we use the following parameters: $N = 100$, $Ro = 0.0548$, $Pr = 1$, $Ra = 1$, $\Delta t = 0.1$ and a final time $t = 1$. Figure 4.8 to Figure 4.11 show the numerical unsteady solution compared to the analytical solution for T, ζ, ψ, and u respectively.

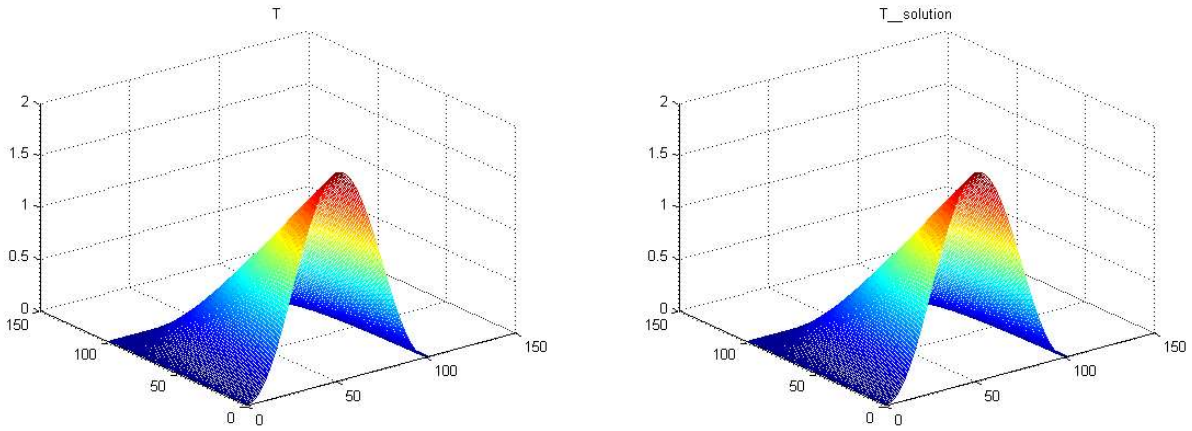

Figure 4.8: (Left): Numerical unsteady solution for T of approximate equations. (Right): Analytical unsteady solution for T of approximate equations.

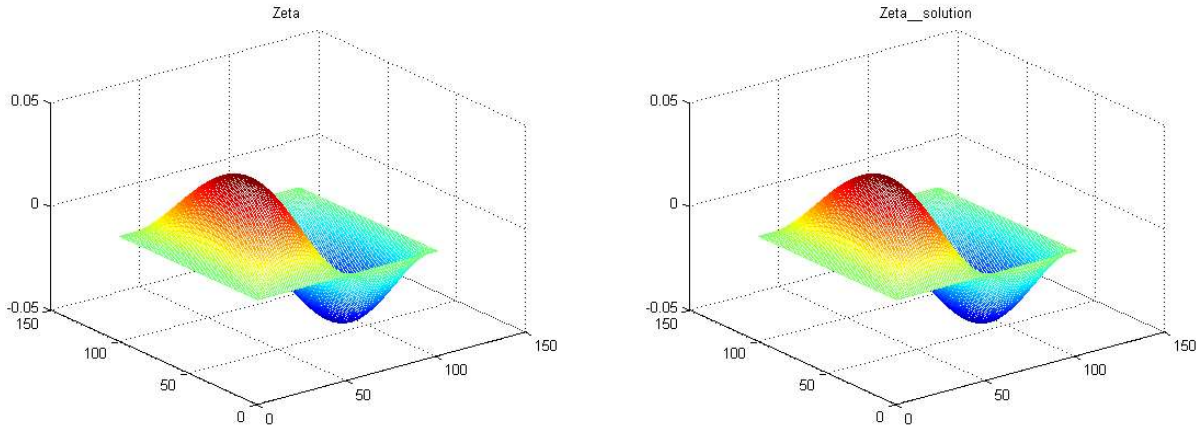

Figure 4.9: (Left): Numerical unsteady solution for ζ of approximate equations. (Right): Analytical unsteady solution for ζ of approximate equations.

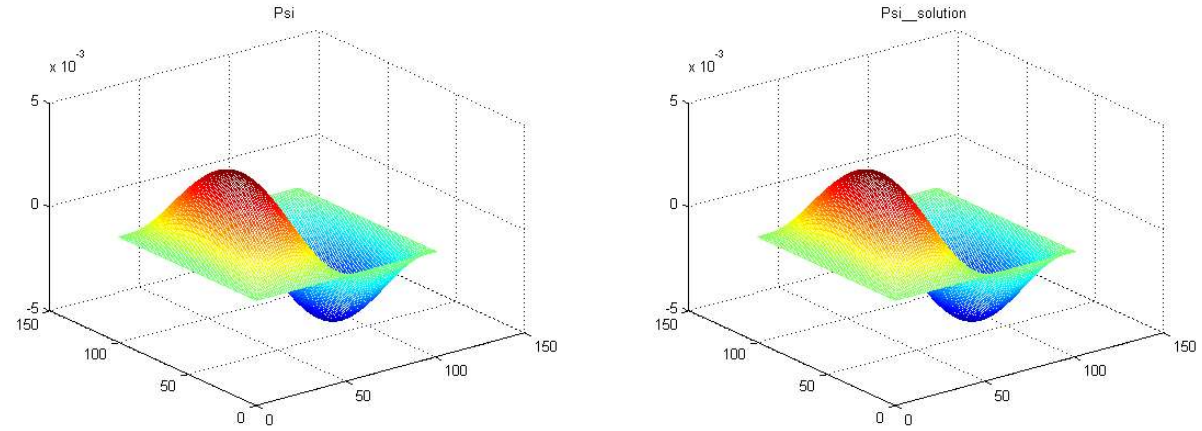

Figure 4.10: (Left): Numerical unsteady solution for ψ of approximate equations. (Right): Analytical unsteady solution for ψ of approximate equations.

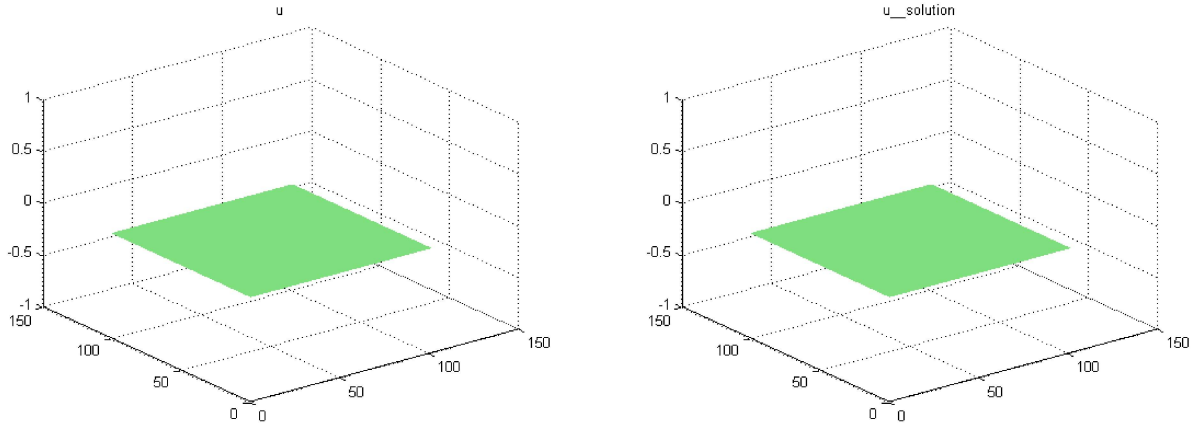

Figure 4.11: (Left): Numerical unsteady solution for u of approximate equations. (Right): Analytical unsteady solution for u of approximate equations.

Table 4.2 shows the error calculated with varying grid sizes by using the same way defined in (4.1). Similarly to the steady state case, the numerical unsteady solutions for T are also the exact solution. We get second order convergence for ψ and ζ, of which $\frac{E_{2h}}{E_h}$ is approximately 4. The results are consistent with the error arising from the finite difference method we have discussed in the previous chapter (3.6) to (3.9).

grid size (h)	T		ζ		ψ	
	E_h	$\frac{E_{2h}}{E_h}$	E_h	$\frac{E_{2h}}{E_h}$	E_h	$\frac{E_{2h}}{E_h}$
$\frac{1}{10}$	0.2219×10^{-13}	$--$	0.0025	$--$	0.2219×10^{-3}	$--$
$\frac{1}{20}$	0.0178×10^{-13}	0.1250	0.0007	3.7567	0.0591×10^{-3}	3.7559
$\frac{1}{40}$	0.0466×10^{-13}	0.3810	0.0002	4.0134	0.0150×10^{-3}	3.9475
$\frac{1}{80}$	0.1799×10^{-13}	0.2593	0.0000	4.1512	0.0039×10^{-3}	3.8319

Table 4.2: Error table for numerical unsteady solutions of approximate problem.

4.3 Numerical unsteady solutions of full set of original nonlinear equations

In this experiment, we use the following parameters: $N = 100$, $Ro = 0.0548$, $Pr = 1$, $Ra = 1$, $\delta = 0.1$, $\Delta t = 0.01$ and a final time $t = 1$. Figure 4.12 to Figure 4.13 show the numerical unsteady solution for T, ζ, ψ, and u, respectively.

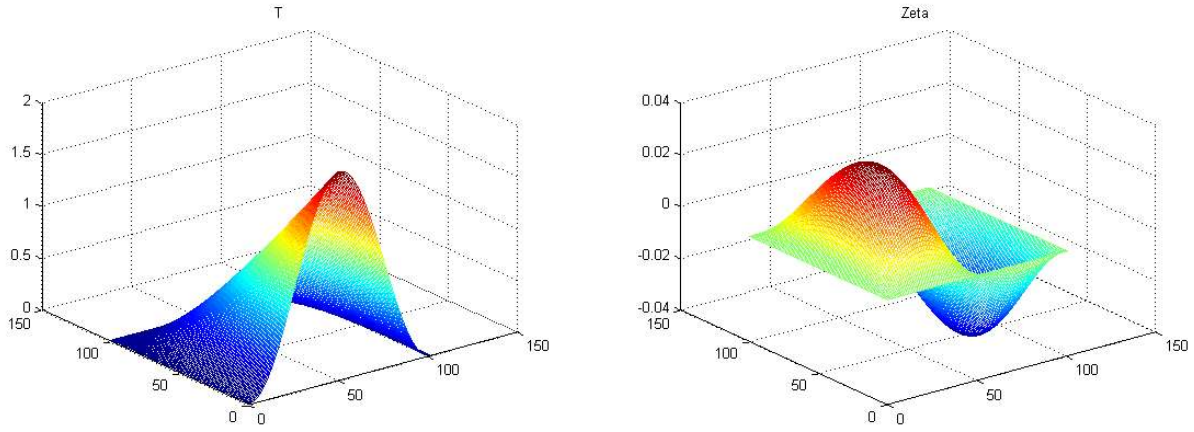

Figure 4.12: (Left): Numerical unsteady solution for T of original nonlinear equations. (Right): Numerical unsteady solution for ζ of original nonlinear equations.

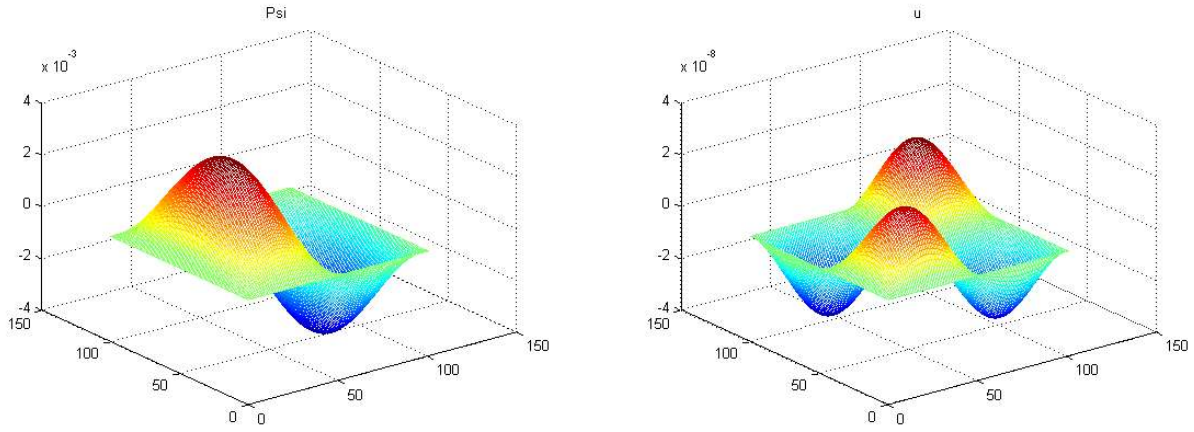

Figure 4.13: (Left): Numerical unsteady solution for ψ of original nonlinear equations. (Right): Numerical unsteady solution for u of original nonlinear equations.

Table 4.3 displays the error calculated with varying grid sizes by defining $E(T)_h = \|T_h - T_{2h}\|_\infty$, $E(\psi)_h = \|\psi_h - \psi_{2h}\|_\infty$ and $E(\zeta_h) = \|\zeta_h - \zeta_{2h}\|_\infty$. The reason why we use a different way of calculating the errors here is that we do not have analytical solutions for the full set of original equations. We can see from the table $\frac{E_{2h}}{E_h}$ is approximately 4 for ζ and ψ. This demonstrates second order convergence, which is consistent with the error arising from the finite difference method we have discussed in the previous chapter (3.6) to (3.9). But the errors of T and u are worse than second order. The possible reason maybe because the Δt we use here is 0.1, which results in that the first order time stepping error dominates the error. Thus, they do not show second order convergence.

grid size (h)	T		ζ		ψ		u	
	E_h	$\frac{E_{2h}}{E_h}$	E_h	$\frac{E_{2h}}{E_h}$	E_h	$\frac{E_{2h}}{E_h}$	E_h	$\frac{E_{2h}}{E_h}$
$\frac{1}{5}$	$--$	$--$	$--$	$--$	$--$	$--$	$--$	$--$
$\frac{1}{10}$	0.0010	$--$	0.0058	$--$	0.1663×10^{-3}	$--$	0.1663×10^{-6}	$--$
$\frac{1}{20}$	0.0011	0.8858	0.0016	3.5418	0.1228×10^{-3}	3.4667	0.1228×10^{-6}	1.3549
$\frac{1}{40}$	0.0006	1.7984	0.0004	3.7763	0.0708×10^{-3}	3.8071	0.0708×10^{-6}	1.7344
$\frac{1}{80}$	0.0002	2.9966	0.0001	3.9750	0.0363×10^{-3}	3.9796	0.0363×10^{-6}	1.9503

Table 4.3: Error table for numerical unsteady solutions of original nonlinear equations.

4.4 Bénard instability

It has been shown [9] that if Ra is smaller than a certain critical value, then there will be no convection, due to the stabilizing effect of the viscosity. But if Ra is larger than the critical value, then convection will occur. In this experiment, we focus on the traditional Bénard problem which has a constant temperature on the boundary. The theoretical critical Ra value is given as $Ra = \frac{27\pi^4}{8}$, which is approximately $Ra = 329$. We display the the stream function for the equations (2.5) to (2.8) with boundary conditions (2.9) to show the evolution of convection with increasing Ra values. In the following experiments, we use $Ro = 0.0548$, $Pr = 0.7046$, $\delta = 0.1$, $N = 80$.

First, we set $Ra = 1$. Figure 4.14 shows that there is no convection when $Ra = 1$, since the magnitude of ψ is about 5×10^{-5}. It can be considered to be negligible.

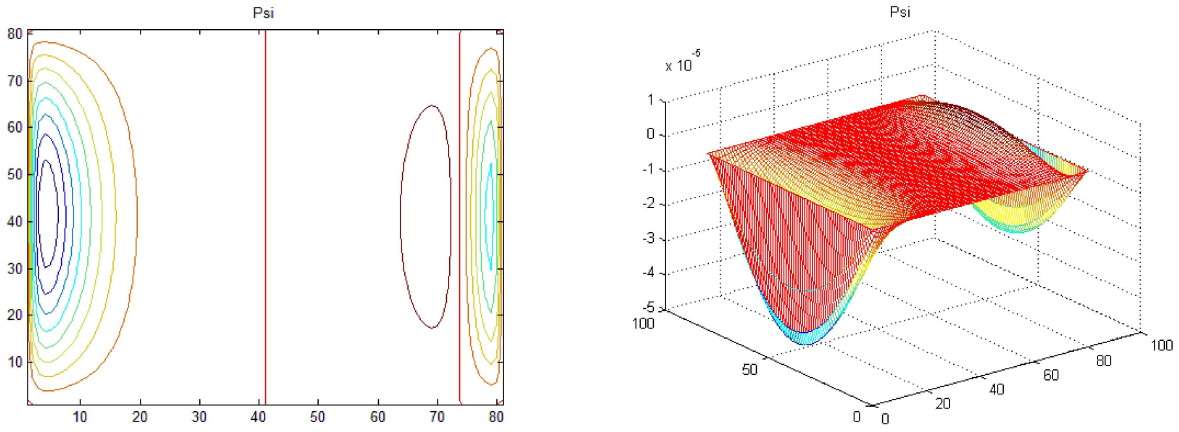

Figure 4.14: (Left): Contour plot of ψ when $Ra = 1$. (Right): Mesh plot of ψ when $Ra = 1$.

Second, we set $Ra = 200$. Figure 4.15 illustrates weak convection when $Ra = 200$. In other words, no significant flow occurs when $Ra = 200$.

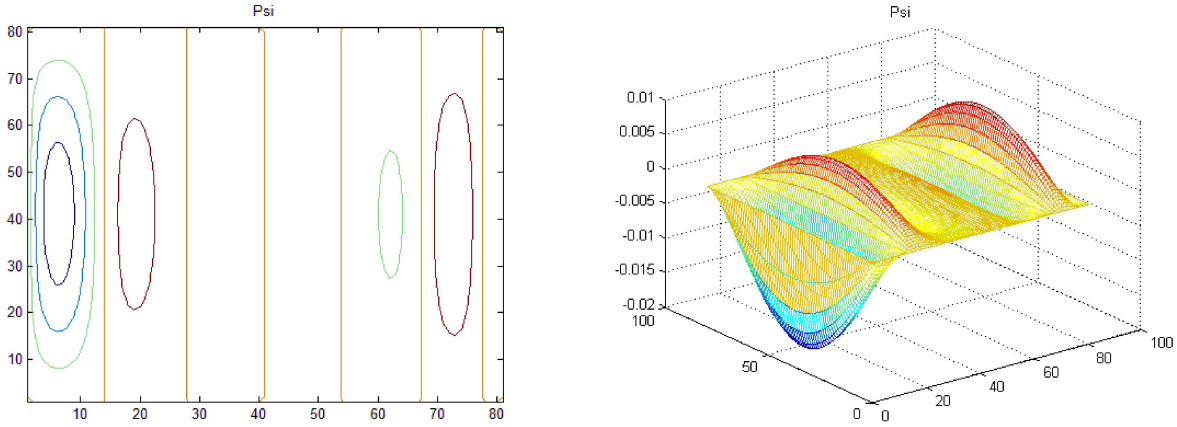

Figure 4.15: (Left): Contour plot of ψ when $Ra = 200$. (Right): Mesh plot of ψ when $Ra = 200$.

Third, we set $Ra = 300$ which is still slightly smaller than the critical value. Figure 4.16 shows that when Ra approaches to the theoretical critical value of $Ra = 329$, convection gets stronger.

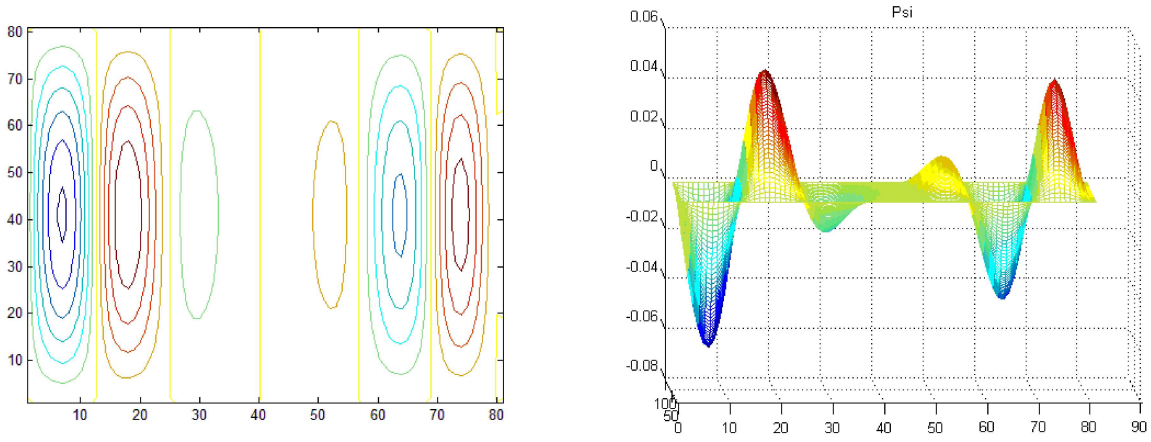

Figure 4.16: (Left): Contour plot of ψ when $Ra = 300$. (Right): Mesh plot of ψ when $Ra = 300$.

Then, we set $Ra = 350$ which is just beyond the critical value. Figure 4.17 illustrates that we get noticeable convection for $Ra = 350$.

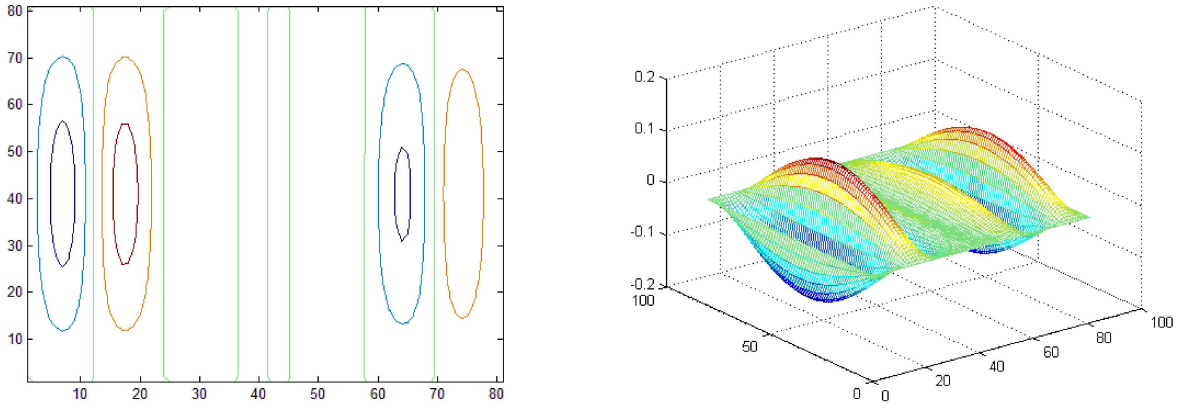

Figure 4.17: (Left): Contour plot of ψ when $Ra = 350$. (Right): Mesh plot of ψ when $Ra = 350$.

Next, Ra is increased to 400. According to the increased number of convection cells and increase in magnitude of ψ shown in Figure 4.18, we have stronger convection here than when $Ra = 350$.

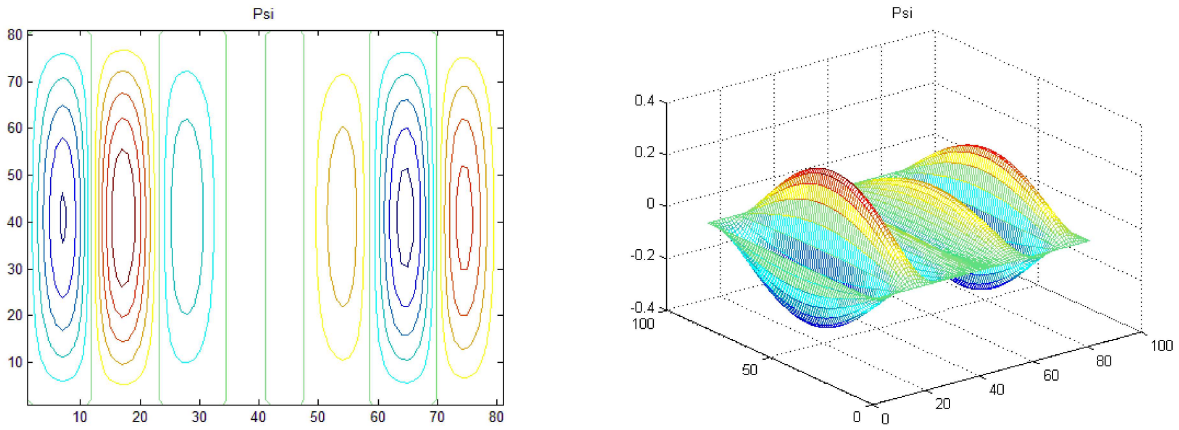

Figure 4.18: (Left): Contour plot of ψ when $Ra = 400$. (Right): Mesh plot of ψ when $Ra = 400$.

Lastly, we set $Ra = 450$. The stream function ψ in Figure 4.19 exhibits an even stronger flow than in the previous cases.

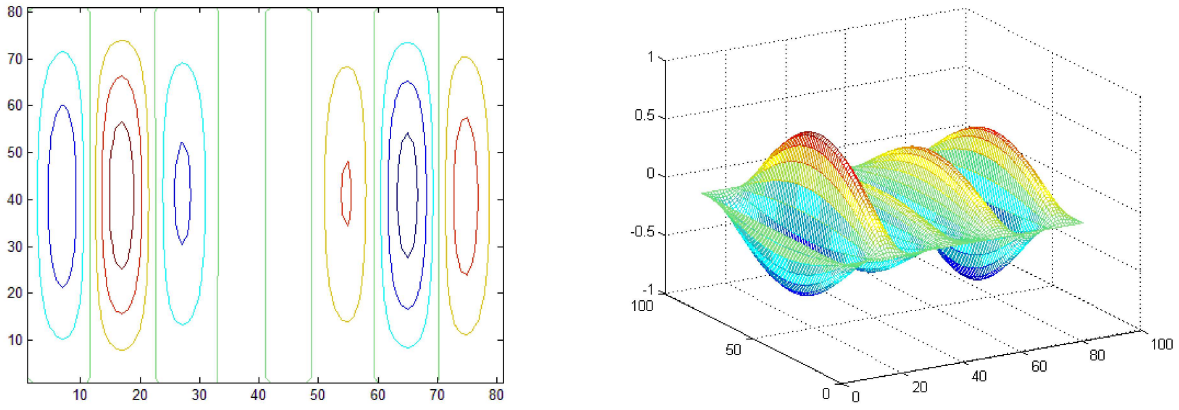

Figure 4.19: (Left): Contour plot of ψ when $Ra = 450$. (Right): Mesh plot of ψ when $Ra = 450$.

Chapter 5

Conclusion

In this paper, we investigated the Rayleigh-Bénard problem with rotation and a periodic temperature distribution. We presented numerical steady-state and unsteady solutions to the approximate and full equations. The numerical results are based on a finite difference method, an implicit time stepping method and an iteration algorithm.

From comparisons with the analytical solutions to the approximate equations, we showed that the numerical results are in good agreement. The numerical results demonstrated second order convergence which is consistent with the finite difference method applied.

We performed numerical experiments by varying the Rayleigh number. The experiments confirmed the theoretical prediction for the onset of convection.

In this work, we only considered a simplified version of our original problem. The simplified model was intended to mimic the flow in the atmosphere. Instead we considered the flow in a confined long, rotating rectangular domain with a sinusoidally varying temperature along the bottom. Possible future work includes transforming the plates to curved surfaces. And then, investigating the Rayleigh-Bénard problem with rotation and a periodic temperature distribution on the curved surfaces.

References

[1] E. Bodenschatz, W. Pesch, and G. Ahlers. Recent developments in Rayleigh-Bénard convection. *Annu. Rev. Fluid Mech.*, 32:709–778, 2000.

[2] H. Bénard. Les tourbillons cellulaires dans une mappe liquide. *Rev. Gen. Sci. Pures Appl.*, 11:1261–71, 1990.

[3] G. Freund, W. Pesch, and W. Zimmermann. Rayleigh–Bénard convection in the presence of spatial temperature modulations. *J. Fluid Mech.*, 673:318–348, 2011.

[4] S.J.D. D'Alessio and K.A. Ogden. Bénard convection with rotation and a periodic temperature distribution. In *M. Rahman and C.A. Brebbia (editors), Advances in Fluid Mechanics IX*, volume 74, pages 453–463. WIT press, 2012.

[5] P. K. Kundu. *Fluid Mechanics.* Academic Press, Inc., third edition, 2004.

[6] R. J. LeVeque. *Finite Difference Methods for Ordinary and Partial Differential Equations: Steady-State and Time-Dependent Problems (Classics in Applied Mathematic).* Society for Industrial and Applied Mathematics, 2007.

[7] M. J. Baines and K. W. Morton. *Numerical Methods for Fluid Dynamics.* Clarendon Press, 1994.

[8] D. C. Hanselman and B. L. Littlefield. *Mastering MATLAB.* Prentice Hall, 2011.

[9] P. G. Drazin and W. H. Reid. *Hydrodynamic Stability.* Cambridge University Press, second edition, 2004.